Solar Physics (2004) 224: 255–268

THE TEMPERATURE OF THE LOW CORONA DURING SOLAR CYCLES 21–23*

RICHARD C. ALTROCK
Air Force Research Laboratory, Space Vehicles Directorate, National Solar Observatory at Sacramento Peak, P.O. Box 62, Sunspot, NM 88349-0062, U.S.A.
(e-mail: altrock@nso.edu)

(Received 6 September 2004; accepted 14 October 2004)

Abstract. Observations of the forbidden coronal lines Fe XIV 530.3 nm and Fe X 637.4 nm obtained at the National Solar Observatory at Sacramento Peak are used to determine the variation of coronal temperature at latitudes above 30° during solar activity cycles 21–23. Features of the long-term variation of emission in the two lines are also discussed. Temperatures at latitudes below 30° are not studied because the technique used to determine the coronal temperature is not applicable in active regions. The polar temperature varies cyclically from approximately 1.3 to 1.7 MK. The temperatures are similar in both hemispheres. The temperature near solar minimum decreases strongly from mid-latitudes to the poles. The temperature of the corona above 80° latitude generally follows the sunspot cycle, with minima in 1985 and 1995–1996 (cf. 1986 and 1996 for the smoothed sunspot number, Rz) and maxima in 1989 and 2000 (cf. 1989 and 2000 for Rz). The temperature of the corona above 30° latitude at solar maximum is nearly uniform, i.e., there is little latitude dependence. If the maximum temperatures of cycles 22 and 23 are aligned in time (superposed epochs), the average annual N + S temperature (average of the northern and southern hemisphere) in cycle 23 is hotter than that in cycle 22 at all times both above 80° latitude and above 30° latitude. The difference in the average annual N + S maximum temperature between cycles 23 and 22 was 56 kK near the poles and 64 kK for all latitudes above 30°. Cycle 23 was also hotter at mid-latitudes than cycle 22 by 60 kK. The last 3 years of cycle 21 were hotter than the last 3 years of cycle 22. The difference in average annual N + S temperatures at the end of cycles 21 and 22 was 32 kK near the poles and 23 kK for all latitudes above 30°. Cycle 21 was also hotter at mid-latitudes than cycle 22 by at least 90 kK. Thus, there does not seem to be a solar-cycle trend in the low-coronal temperature outside of active regions.

1. Introduction

The solar coronal temperature may be calculated as a function of the ratio of absolute intensities of the visible Fe XIV (530.3 nm "green") and Fe X (637.4 nm "red") lines, which was discussed as far back as the 1950s (cf., Noci, 2003) and more recently by Guhathakurta, Fisher and Altrock (1993). The latter paper shows that this technique is insensitive to errors in absolute calibration; an order of magnitude error in the ratio of the intensities only results in a 12% error in the temperature. In that paper we showed that there is a tendency for higher coronal temperatures to follow the photospheric magnetic neutral line at high latitudes. Altrock *et al.* (1996), Hick *et al.* (1996) and Hick, Jackson and Altrock (1996) further found a correlation

between high coronal temperatures and magnetic neutral lines at lower latitudes. Hick, Jackson and Altrock (1996) also found a suggestion for the epochs analyzed that the large-scale higher-latitude temperatures have a tendency to be independent of height, if individual "hot spots" are ignored.

Makarov and Tlatov (2002) performed a long-term study of the large-scale green/red-ratio temperature, and concluded that the polar zones of the the lower corona decreased in temperature by approximately 100 kK over the last 50 years. Altrock (1998) displayed the first synoptic maps of green/red temperature covering over one solar cycle. In this paper, I use this technique to study the long-term, large-scale variation of temperature in the corona over the last two solar cycles.

2. Observations

The observations are described by Altrock (1997). They consist of latitude scans of the corona every 3° at 1.15 solar radii ($R_{\odot}$) in the green and red lines. The scans were obtained at the John W. Evans Solar Facility of the National Solar Observatory at Sacramento Peak from 1983 through 2002 with the photoelectric coronal photometer and the 40-cm coronagraph (Fisher, 1973, 1974; Smartt, 1982).

3. Procedure

The scans are calibrated to absolute intensity, and suitable temporal averages are taken to reduce noise. The ratios of the green and red intensities are converted to temperature and searched for long-term trends during solar cycles 21–23. Only data obtained outside of the active-region zones (±30°) are used, because this technique is not applicable in active regions, where the requirement of a uniform temperature along the line of sight (LOS) is denied by the presence of many loops of different temperatures. At higher latitudes where active regions do not occur, the LOS above the limb passes through regions of uniform temperature defined by individual coronal streamers.

4. Coronal Intensity

Figure 1 (top) shows a synoptic plot of intensity in the green line at $r = 1.15\ R_{\odot}$ from 1983 through 2002. Earlier scans obtained in this line from 1976 through 1982 are not shown in order to focus attention on the last two solar cycles, for which we have data in both lines. Clearly visible is the coronal activity associated with cycles 22 and 23, descending from approximately 30° latitude to the equator. Also visible are the extensions of coronal activity to the poles, connected with the "rush to the poles" originally seen in polar-crown prominences around the time of solar maximum and seen here in the overlying coronal streamers. Solar maxima (maximum of

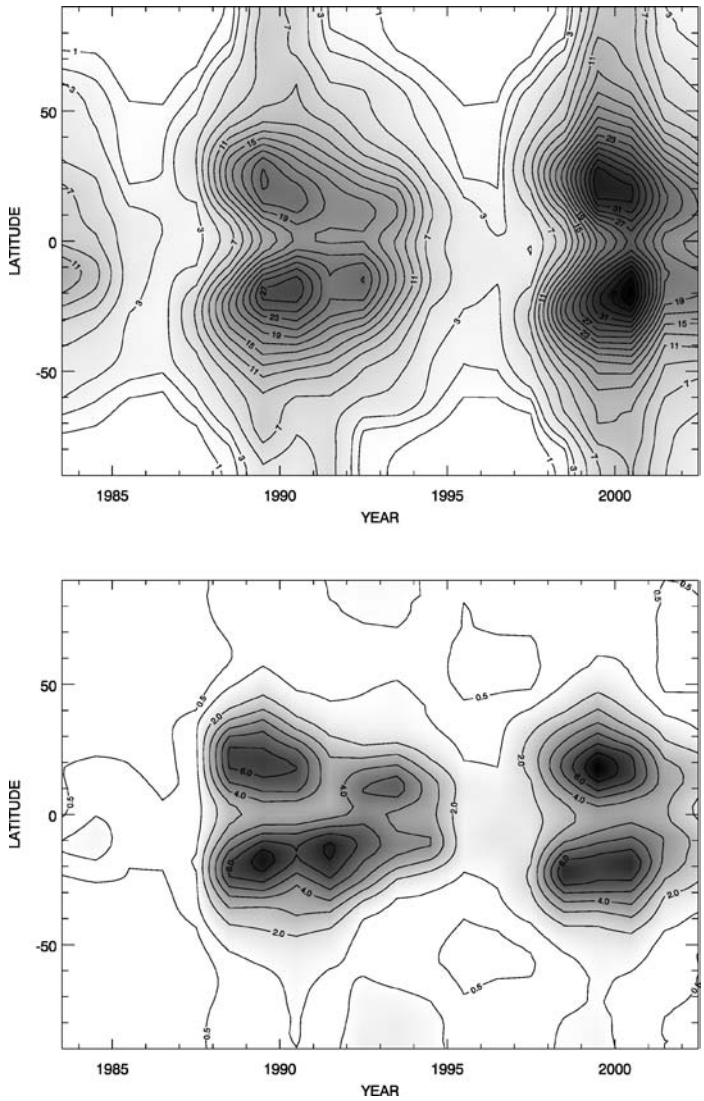

Figure 1. Top: contours of annual averages of coronal intensity in Fe XIV 530.3 nm at a height of 0.15 solar radii ($R_\odot$) above the solar limb plotted versus time and latitude from 1983 through 2002. The units are millionths of the brightness of the solar disk at the given wavelength. *Bottom*: as given earlier but for Fe X 637.4 nm.

the smoothed sunspot number, Rz, as calculated by the NOAA National Geophysical Data Center) occur at 1989.6 and 2000.3. Solar minima occur at 1986.8 and 1996.4.

Observations in the red line began in 1983. Figure 1 (bottom) shows a synoptic plot for this line. Solar cycles 22 and 23 are again clearly seen. The extensions to the poles seen in the green line near solar maximum are much weaker here and are not

seen above 50° latitude in the northern hemisphere. However, there are unexpected episodes of weak emission at and near the poles after solar maximum (cf., 1991 into 1994 and possibly in the mid-1980s and again beginning in 2001). They occur during the phase of the solar cycle in which large coronal holes form at the poles and extend down to lower latitudes. This emission could be the signature of these lower-temperature phenomena.

Symmetric regions of red emission are also seen in mid-latitudes from 1995 to 1997 and possibly 11 years earlier. Perhaps these are also connected with late-cycle coronal holes.

5. The Morphology of Coronal Temperature Patterns

Since *Rz* maxima and minima are defined by 12-month running means, it seems appropriate to compare *Rz* to annual averages of temperature. Figure 2 shows annual averages of coronal temperature in MK (millions of kelvins) calculated by dividing the intensities shown in Figure 1 (top) by those in Figure 1 (bottom), as discussed in Section 1. This method does not give reliable temperatures over active regions

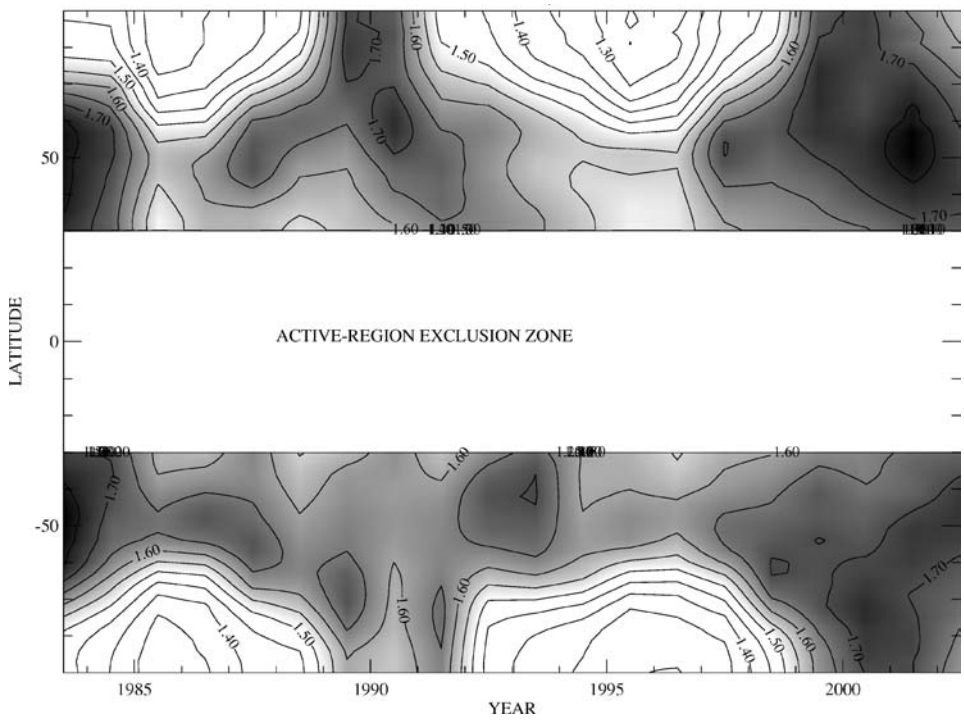

Figure 2. Contours of annual averages of coronal temperature at a height of 0.15 $R_{\odot}$ above the solar limb plotted versus time and latitude from 1983 through 2002. See text for discussion of the active-region exclusion zone. The units are millions of kelvins (MK).

due to their complexity (cf., Altrock *et al*., 1996); hence, the region from +30 to −30° latitude, where the vast majority of active regions occur, is not considered. Outside of this active-region exclusion zone we see a striking pattern of solar-cycle variation of higher-latitude coronal temperature.

High temperatures are first seen at middle latitudes in 1983 preceding solar minimum. Approaching solar minimum, a wave of cooler temperature develops near the poles and progresses towards lower latitudes as the poles become even cooler. By the time of solar minimum, the zone of higher temperatures is confined to latitudes below about 50°, and maximum cooling is occurring at the poles. Shortly after solar minimum, a wave of high temperatures moves poleward from the mid-latitude warm zone and reaches the poles around solar maximum. A region of high temperatures persists at the poles for a couple of years and then begins to gradually cool. At this point, the wave of cooler temperatures begins its equatorward motion again, as the solar-cycle pattern follows its earlier progression.

The overall pattern is approximately symmetric, both in time relative to the phase of the solar cycle and in latitude about the equator. Penn *et al*. (1998) suggest that this pattern may be due to the cancellation of magnetic flux. The proximity of the poleward-moving hot wave to the the "rush to the poles" suggests a correlation with the magnetic reconnection that is occurring in the polar crown.

The amplitude of this pattern in the polar regions is given in Table I. Beginning with solar minima, the polar temperature at the end of cycle 21 is 1.31 MK in 1985, and at the end of cycle 22 it is 1.24 MK at the north pole in 1995 and 1.30 MK at the south pole in 1995 and 1996 (note that the *Rz* minima occur in 1986 and 1996). As the solar cycle progresses, the polar temperature rises and reaches maxima of 1.72 MK in the north in 1989 and 1.66 MK in the south in 1991. An earlier secondary maximum in the south occurred in 1989 at 1.63 MK. *Rz* maximum occurred in 1989.

In cycle 23 the temperature at the north pole maximizes at 1.71–1.72 MK in 1999–2000. At the south pole, maxima also occur at 1.71–1.72 MK in 2000–2001. *Rz* maximum occurs in 2000.

5.1. Average of the North and South Hemispheres

Since the pattern and amplitude is similar in both hemispheres it is reasonable to reduce noise by averaging the results from the north and south hemispheres. Figure 3 shows the north + south average of Figure 2. This will increase the signal-to-noise ratio for any features that are symmetrical about the equator, and all of the features of Figure 2 appear very clearly in Figure 3.

The amplitude in the polar regions of Figure 3 is also given in Table I. Beginning with solar minima, the minimum polar temperature at the end of cycle 21 is 1.31 MK in 1985, and at the end of cycle 22 it is 1.28–1.29 MK in 1995–1996. At the maximum of cycle 22 the temperature at the poles reaches 1.67 MK in 1989. In cycle 23 the temperature maximized at 1.72 MK in 2000.

TABLE I

Maxima and minima of *Rz* and annual-average coronal temperatures in MK above 80° latitude for solar cycles 22 and 23.

min	yr	max	yr	rise	fall
		Cycle 22			
Rz					
12.3	1986.8	158.5	1989.6	2.8	6.8
North-polar temperature					
1.31	1985	1.72	1989	4	6
South-polar temperature					
1.31	1985	1.63	1989	4	6, 7
		1.66	1991	6	4, 5
North + south average polar temperature					
1.31	1985	1.67	1989	4	6, 7
		Cycle 23			
Rz					
8.0	1996.4	120.8	2000.3	4.0	
North-polar temperature					
1.24	1995	1.71	1999	4	
		1.72	2000	5	
South-polar temperature					
1.30	1995	1.72	2000	5, 6	
1.30	1996	1.71	2001	4, 5	
North + south average polar temperature					
1.28	1995	1.72	2000	4, 5	
1.29	1996				

max: maximum value of the parameter (in some cases there are two maxima).
min: minimum value of the parameter (in some cases there are two minima).
yr: year of the minimum or maximum in the preceding column.
rise: time in years to go from minimum to maximum for the parameter.
fall: time in years to go from maximum to minimum for the parameter.
Rz: smoothed sunspot number.

The amplitude of this pattern at a middle latitude (54°) is given in Table II. The hottest temperatures seen anywhere on Figure 3 occur in the middle latitudes around solar maximum. In 1983 the temperature reaches 1.78 MK at 54°, which is the maximum temperature on the map. During the cooling phase that follows, the temperature at that latitude decreases to 1.60 MK in 1985. The next heating phase at mid-latitudes is not as strong as that in cycle 21. The maximum temperature at 54° is 1.69 MK in 1987. In 1996 the temperature there falls to 1.56 MK. Strong mid-latitude heating returns in cycle 23, reaching 1.75 MK in 2001.

TABLE II

Maxima and minima of north + south annual-average coronal temperatures in MK at 54° latitude for solar cycles 21–23.

Cycle	Minimum	Year	Maximum	Year
21			1.78	1983
22	1.60	1985	1.69	1987
23	1.56	1996	1.75	2001

Year: year of the minimum or maximum in the preceding column.

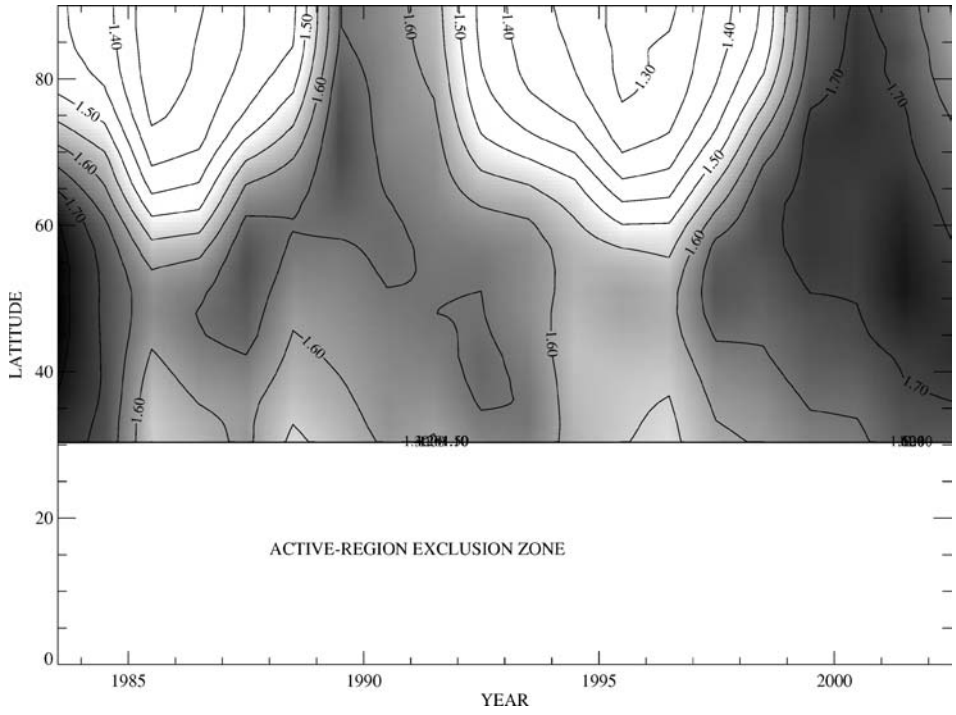

Figure 3. As in Figure 2, but with the northern and southern hemispheres averaged together.

5.1.1. *The symmetry of the temperature cycle relative to that of the sunspot cycle*

For simplicity here we confine our discussion to the N + S (average of north plus south hemispheres) results of Table I. The reader is invited to analyze the more complex results of the separate hemispheres, which, on average, yield the same results. Table I shows that (i) polar temperature minimum occurs at or slightly before *Rz* minimum, and (ii) polar temperature maximum occurs at *Rz* maximum. Thus, on average, the polar temperature increased slower (longer rise time) than *Rz*, as shown

in the "rise" column. Since the temperature cycle appears to be related to the activity cycle, we may assume that, on average, the temperature- and activity-cycle lengths are the same (this is shown to be approximately true in Table I by calculating the "min to min" and "max to max" cycle lengths). If so, this would imply a shorter fall time for the polar temperature relative to Rz (for cycle 22 the result is inconclusive in

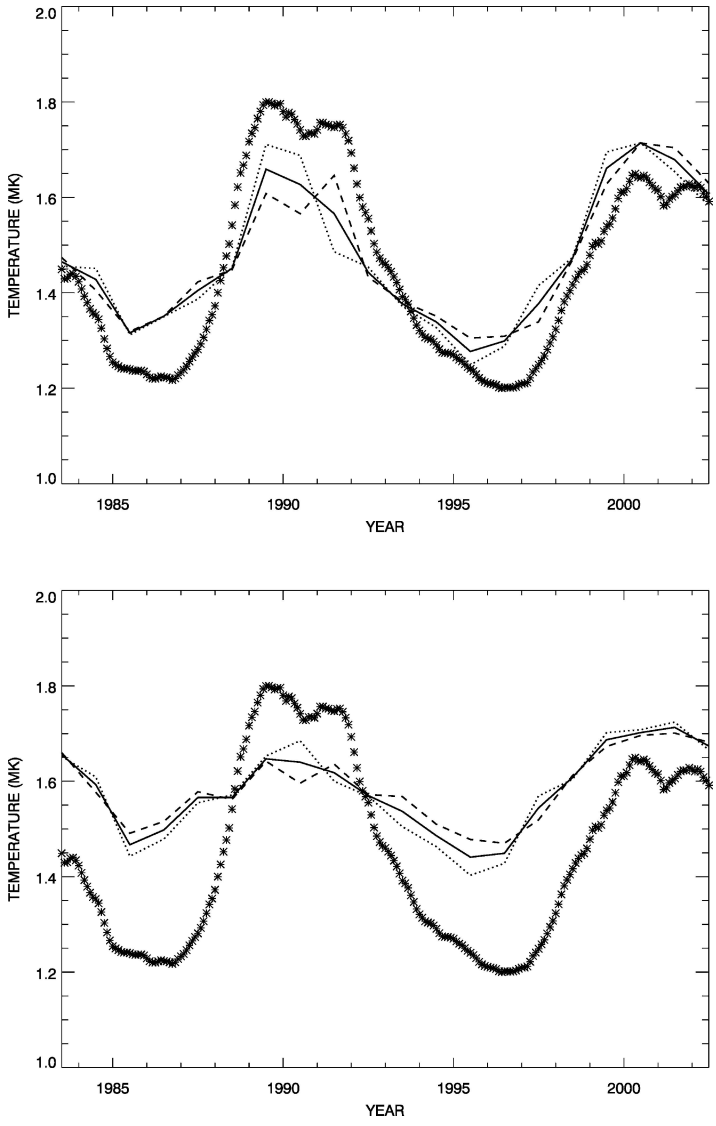

Figure 4. *Top*: Annual-average coronal temperature above 80° latitude. *Dots*: northern hemisphere. *Dashes*: southern hemisphere. *Solid*: N + S average (average of the northern and southern hemisphere). The smoothed sunspot number is shown as *asterisks* on an arbitrary scale. *Bottom*: as given earlier, but for all latitudes above 30°.

the "fall" column). Thus, on average, the polar temperature cycle is more symmetric than the *Rz* cycle: the rise and fall times are more nearly equal than for *Rz*.

6. A Detailed Comparison of Coronal Temperatures for Solar Cycles 21–23

Tables I and II give evidence that, in the corona, solar cycles 21 and 23 were hotter than cycle 22. We will explore this further in this section.

Figure 4 (top) shows the variation of temperature with time for latitudes above 80°, obtained from the results of Figures 2 and 3. A clear solar-cycle variation is seen, nearly in phase with the sunspot cycle. It is clear that the variations in each hemisphere are very similar.

Figure 4 (bottom) shows similar results for all latitudes above 30°. We see that including lower latitudes raises the temperature at solar minimum, but the temperature at solar maximum is very similar to the high-latitude case. Thus, the temperature near solar maximum is nearly uniform over the entire corona above 30° latitude. Again the variations of the north and south hemispheres are very similar.

Figure 5 shows a superposition of only the N + S average curves from Figure 4. The lower-latitude temperatures are significantly higher than those at high latitudes

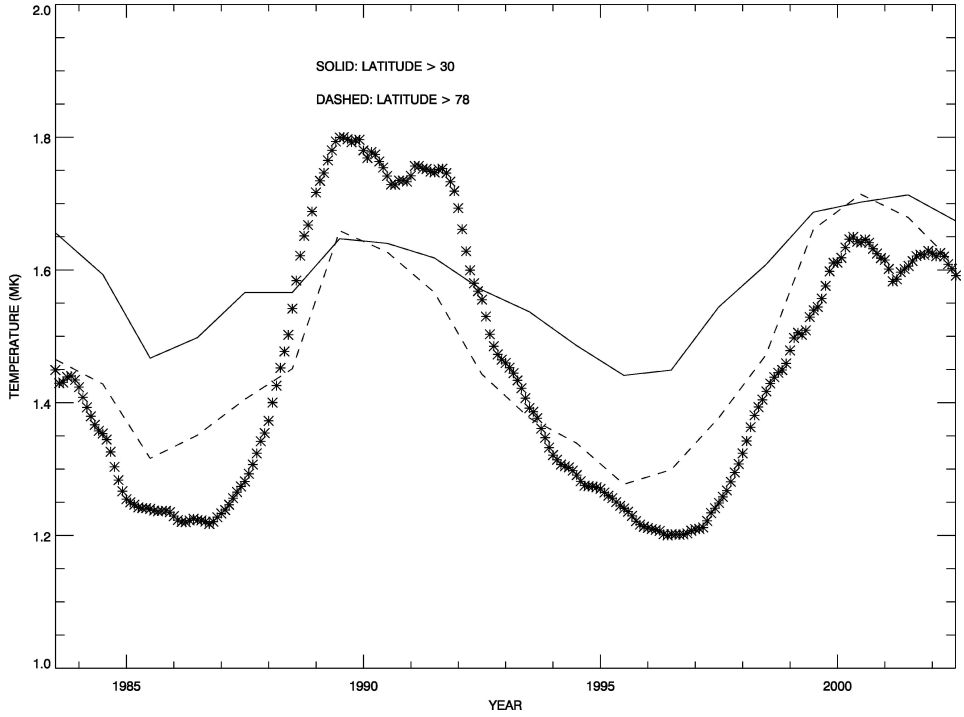

Figure 5. Annual-average coronal temperature. *Dashed*: above 80° latitude. *Solid*: above 30° latitude. The smoothed sunspot number is shown as *asterisks* on an arbitrary scale.

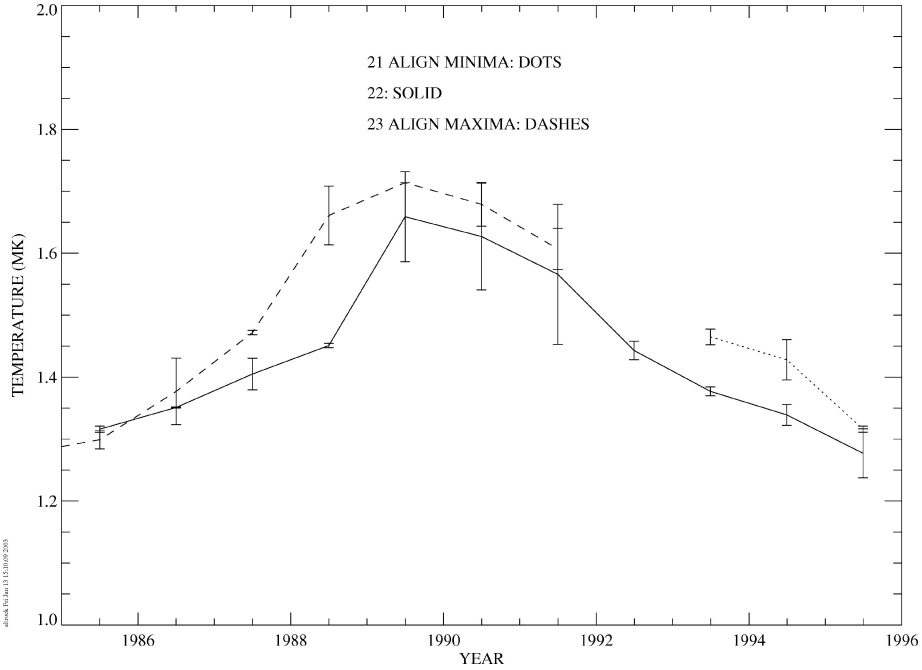

Figure 6. Superposed epoch analysis of annual-average coronal temperature above 80° latitude versus year of cycle 22. *Solid*: cycle 22. *Dots*: cycle 21 shifted to align minimum with that of cycle 22. *Dashes*: cycle 23 shifted to align maximum with that of cycle 22. Uncertainty bars show the range of values from the northern and southern hemispheres.

at solar minimum, but at solar maximum the lower-latitude temperature is very similar to the high-latitude case. Thus, the temperature near solar maximum is nearly uniform over the entire corona above 30° latitude.

Figures 6 and 7 show superposed epoch analyses of the curves of Figure 5. Here we can see a comparison of the entire solar-cycle variation of coronal temperature for cycles 21–23. Cycle 23 has obviously been hotter than 22 for the epochs analyzed. However, cycle 21 appears to have been hotter than cycle 22, although we have only 3 years of data for cycle 21. This would argue against any monotonic increase in the cycle-averaged coronal temperature.

7. Conclusions

Observations at 1.15 solar radii of the forbidden coronal lines Fe XIV 530.3 nm and Fe X 637.4 nm obtained at the National Solar Observatory at Sacramento Peak were used to determine the variation of coronal temperature at middle and high latitudes during parts or all of solar cycles 21–23.

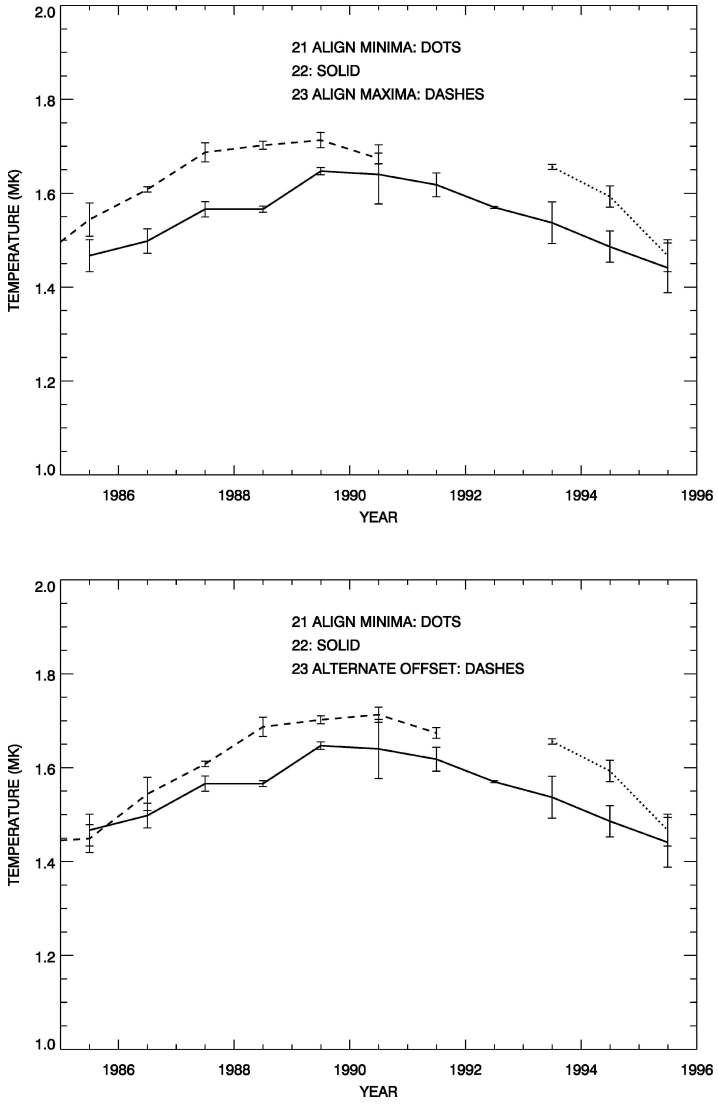

Figure 7. As in Figure 6, but for latitudes above 30°. *Top*: cycle 23 shifted to align maximum with that of cycle 22. *Bottom*: An alternate shift of cycle 23 that may be more suitable, in that the two curves are more congruent.

Coronal emission generally follows the sunspot cycle at low latitudes. Fe XIV has significant high-latitude emission near solar maximum. Fe X high-latitude emission near solar maximum is weaker. Also in Fe X, there are unexpected episodes of weak emission at and near the poles after solar maximum. They occur during the phase of the solar cycle in which large coronal holes form at the poles and extend down to lower latitudes. This emission could be the signature of these lower-temperature

phenomena. Symmetric regions of Fe X emission are also seen in mid-latitudes from 1995 to 1997 and possibly 11 years earlier.

A clear solar-cycle variation of the coronal temperature both near the poles and also for all latitudes above 30° is seen over the 20 years analyzed, nearly in phase with the sunspot cycle. Near the poles the temperature varies from about 1.3 to 1.7 MK. This unexpectedly large-amplitude variation appears in both hemispheres symmetrically, and the temperatures are similar in the two hemispheres.

The temperature near solar minimum decreases strongly from mid-latitudes to the poles, but the temperature of the corona above 30° latitude at solar maximum is nearly uniform, i.e., there is little latitude dependence.

Solar cycle 23 was hotter than solar cycle 22. If the maximum temperatures of cycles 22 and 23 are aligned in time (superposed epochs), the annual N + S (average of the northern and southern hemispheres) average temperature in cycle 23 is hotter than that in cycle 22 (i) at all times above 80° latitude and (ii) at all times above 30° latitude. The maximum temperature during solar cycle 23 was higher than that during solar cycle 22 in annual N + S averages by approximately 0.06 MK both near the poles and at all latitudes above 30°. In addition, the temperature at mid-latitudes was hotter by the same amount during cycle 23 than in cycle 22.

However, cycle 22 may have been cooler than cycle 21 (we have only 3 years of data for cycle 21). The minimum temperature following solar cycle 22 was cooler than that following solar cycle 21. The difference in annual N + S averages was −0.03 MK near the poles and −0.02 MK for all latitudes above 30°. Temperatures during the 3 years of cycle 21 that we have are hotter than those during the last 3 years of cycle 22. In addition, the temperature at mid-latitudes was hotter by at least 0.09 MK during cycle 21 than in cycle 22 . This would argue against any monotonic increase in the coronal temperature as a function of solar-cycle number.

The polar temperature cycle is more symmetric than the *Rz* cycle: the rise and fall times are more nearly equal than for *Rz*.

Appendix: A Critique of a Multiple-Valued Temperature-Determination Technique

Guhathakurta, Fisher and Strong (1996) (referred to as GFS from this point on) studied various coronal emissions over a 2-day period. On the basis of a small amount of data, they conclude that, "... most of the variation in red-(green-) line intensity contrast in polar regions can be explained by density variation alone." However in the samples shown, the red and green intensities are often varying strongly in *opposite* directions in the polar region, which cannot be due to density changes, because both lines have intensities that are positive functions of density. They then note the existence of the very strong anti-correlations in the red and green intensity, which they claim implies that the features are not cospatial. However, the exact same behavior would occur if the features were cospatial but of significantly

different temperatures than the material in adjacent LOS. Thus, there is *no* evidence the intensity variations near the poles are not due to temperature variations between adjacent LOS.

While correctly pointing out that the green/red-ratio technique does not work in regions where there are temperature inhomogeneities along the LOS, such as in active regions, they claim that the technique "... requires accurate knowledge of absolute photometry of the emission-line data..." However, as discussed earlier, the temperature obtained by this technique is only weakly dependent on the ratio of the red and green absolute intensities (cf., Guhathakurta, Fisher and Altrock, 1993).

They next cast doubt on the temperature derived from the green/red ratio by pointing out that both the emissivities and the green/red ratio are double-valued functions of T. However, the emissivity technique, which requires input of density, yields results subject to error due to the use of instruments of different resolutions to observe the density (SXT and Mk III coronagraph) and the line intensities (see Section 2). The green/red-ratio technique is essentially independent of density. Also, for the green/red-ratio technique, Guhathakurta *et al*. (1992) show that, "... one set of solutions has a temperature that is too high for the corona and is therefore eliminated." Thus, the green/red-ratio technique gives a single-valued, density-independent result.

GFS use the densities obtained from white light to obtain two values of the temperature from the double-valued emissivities in the polar regions. For both the red and green lines, they obtain a temperature that matches the line-ratio temperature. That is, within 20° of the poles, the only two emissivity temperatures (one red and one green) that are realistic for coronal holes match *exactly* the green/red-ratio temperature. However, they then conclude that since, "... the polar rays are not cospatial ..." (which we indicated earlier has not been proven) "... the line-ratio technique does not work"! This logic has proven nothing about the validity of the the green/red-ratio technique. What it does prove is that attempting to use the double-valued emissivities technique to determine the temperature for the red and green lines does not produce results capable of clear interpretation, since only two or the four curves yield physically realistic results.

Later, GFS discuss non-polar streamers. They show that the line-ratio technique gives only one result: streamers are hot. However, they also say that their Figure 3 (which uses the double-valued emissivity technique) "... also indicates them to be hot." This is true for *one* of the 4 curves (the red "hot" curve) but *not* for the other 3! Amazingly, the red "hot" curve matches the line-ratio-temperature curve *exactly*! This coincidence is not discussed by the authors. This paragraph does contain the one major conclusion that GFS, Guhathakurta, Fisher, and Altrock (1993) and I agree on and which is crucial to this paper: *"... relatively high temperature in the high-latitude streamers exists practically throughout the solar cycle."*

Other errors exist. They designate one feature ("D") as both a streamer and a "nonradial polar coronal ray." They also say that it is bright in SXT (which it is on

one day but not on the previous day, indicating a rapidly evolving feature) but is "hotter" (no explanation is given for that statement) than the temperature given by the line-ratio technique (which does indicate that it is hot). This may very well be due to activity that occurred at the time of the SXT observation but not at the time of the red and green observations.

In conclusion, GFS uses observations on 2 days of several different features and attempts to prove that the green/red-ratio technique for calculating temperatures is incompatible with the double-valued line-emissivity technique and is therefore wrong. They did not prove their point.

Acknowledgement

The author was supported by the Air Force Office of Scientific Research.

References

Altrock, R. C.: 1997, *Solar Phys.* **170**, 411.

Altrock, R. C.: 1998, in K. S. Balasubramaniam, J. W. Harvey, and D. M. Rabin (eds.), *Synoptic Solar Physics*, 18th NSO/SP Summer Workshop, Sunspot New Mexico, 9–12 September 1997, Astronomical Society of the Pacific, p. 339.

Altrock, R. C., Hick, P., Jackson, B. V., Hoeksema, J. T., Zhao, X. P., Slater, G., and Henry, T. W.: 1996, *Adv. Space Res.* **17**(4/5), 235.

Fisher, R. R.: 1973, *Air Force Cambridge Research Laboratories Technical Reports*, 73-0696.

Fisher, R. R.: 1974, *Solar Phys.* **36**, 343.

Guhathakurta, M., Fisher, R. R., and Altrock, R. C.: 1993, *Astrophys. J. Lett.* **414**, L145.

Guhathakurta, M., Fisher, R. R., and Strong, K.: 1996, *Astrophys. J. Lett.* **471**, L69.

Guhathakurta, M., Rottman, G. J., Fisher, R. R., Orrall, F. Q., and Altrock, R. C.: 1992, *Astrophys. J.* **388**, 633.

Hick, P., Jackson, B. V., and Altrock, R. C.: 1996, in D. Winterhalter, J. T. Gosling, S. R. Habbal, et al. (eds.), *Solar Wind Eight*, Workshop Proceedings, Dana Point, CA, 25–30 June 1995, p. 169.

Hick, P., Jackson, B. V., Altrock, R. C., Slater, G., and Henry, T.: 1996, in K. S. Balasubramaniam, S. L. Keil, and R. N. Smartt (eds.), *Solar Drivers of Interplanetary and Terrestrial Disturbances*, 16th NSO/Sac Peak Workshop, Sunspot, New Mexico, 16–20 October, 1995, Astronomical Society of the Pacific Conference Series, Vol. 95, Astronomical Society of the Pacific, p. 358.

Makarov, V. I. and Tlatov, A. G.: 2002, in Huguette Sawaya-Lacoste (ed.), *Proceedings of the Second Solar Cycle and Space Weather Euroconference*, 24–29 September 2001, Vico Equense, Italy, ESA SP-477, ESA Publications, Noordwijk Division, p. 241.

Noci, G.: 2003, *Memorie della Societa Astronomica Italiana*, **74**, 704.

Penn, M., Altrock, R. C., Henry, T., and Guhathakurta, M.: 1998, in K. S. Balasubramaniam, J. W. Harvey, and D. M. Rabin (eds.), *Synoptic Solar Physics*, 18th NSO/SP Summer Workshop, Sunspot, New Mexico, 9–12 September 1997, Astronomical Society of the Pacific, p. 325.

Smartt, R. N.: 1982, in *Instrumentation in Astronomy IV: Proc. SPIE* **331**, 442.